

**Supporting information for**

**In-situ Twisting for Stabilizing and Toughing Conductive Graphene Yarns†**

Xi Xiang,<sup>a,b</sup> Zhengpeng Yang,<sup>a,c</sup> Jiangtao Di,<sup>a,\*</sup> Wujun Zhang,<sup>a,c</sup> Ru Li,<sup>a</sup> Lixing Kang,<sup>a</sup> Yongyi Zhang,<sup>a,\*</sup>, Haijiao Zhang,<sup>b</sup> Qingwen Li<sup>a,\*</sup>

a. Key Lab of Nano-Devices and Applications, Suzhou Institute of Nano-Tech and Nano-Bionics Chinese Academy of Sciences, Suzhou 215123, China. [jtdi2009@sinano.ac.cn](mailto:jtdi2009@sinano.ac.cn) (J. Di); [yyzhang2011@sinano.ac.cn](mailto:yyzhang2011@sinano.ac.cn) (Y. Zhang); [qwli2007@sinano.ac.cn](mailto:qwli2007@sinano.ac.cn) (Q. Li)

b. School of Environmental and Chemical Engineering, Shanghai University, Shanghai 200444, China

c. Institute of Materials Science and Engineering, Henan Polytechnic University, Jiaozuo 454000, China

## Characterization

Morphology characterization of the investigated samples was performed using SEM (Quanta 400 FEG, FEI) and HRTEM (Tecnai G2 F20 S-Twin, FEI). Raman spectra were collected by a LabRAM HR Raman spectrometer.

## Supporting Figure S1-S9

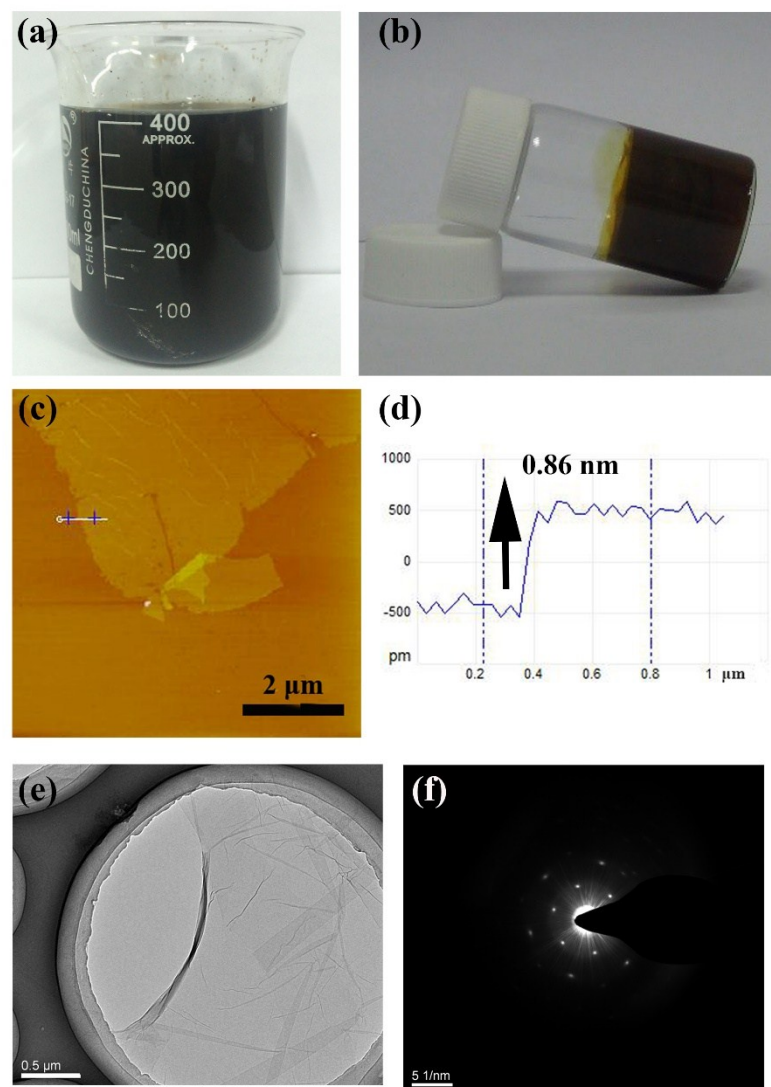


**Figure S1.** Digital images of GO dispersion (a and b). AFM morphology (c) and its height profile (d) of obtained GO sheet, as well as TEM image of GO sheet (e) and the corresponding electron diffraction pattern (f), respectively. The height of GO sheets is 0.86 nm.

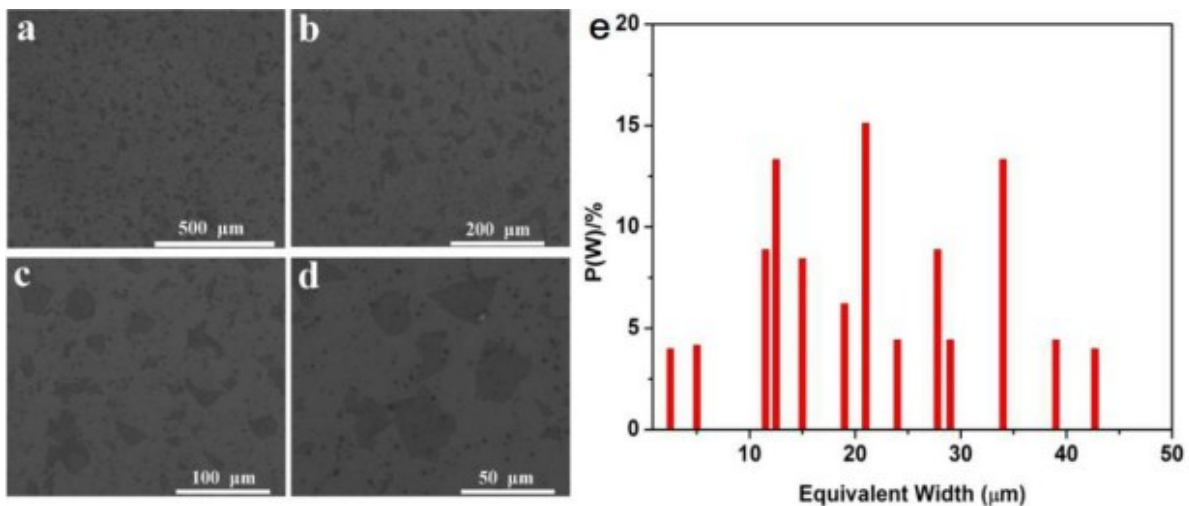


**Figure S2.** SEM images of GO sheets deposited on the silica (a-d). e) The lateral size distribution of GO sheets counted from their SEM images. In the calculation process, the irregular sheets are regarded as squares of equal area and the width of sheets as the side length of squares. The average size of GO sheets is deduced as 21  $\mu\text{m}$ .

raphene fibers could be induced by the tension shear mode, a prevalent mechanism of these GGO and RGO fibers. [30,31] In the neat graphene system, the dominant interactions between graphene and GO sheets are van der Waals interaction, hydrogen bonds and linking. In GGO fibers, the hydrogen bonds contribute to their mechanical strength. In addition, the increasing van der Waals interaction, the increasing interlayer space and the hydrogen bonding interlayer space caused the mechanical properties. Additionally, the oxygen-containing groups on the GGOs can promote their mechanical strength and have resulted from the formation of coordination bonds between the oxygen-containing groups and the carbon atoms of the GO sheets.

**Figure S3.** Photograph of double-plied GO fibers with a continuous alteration of helix angle produced by a double-hole spinneret with a variable rotation speed. The alterable structure of GO fiber indicates the excellent controllability of our fabrication method.

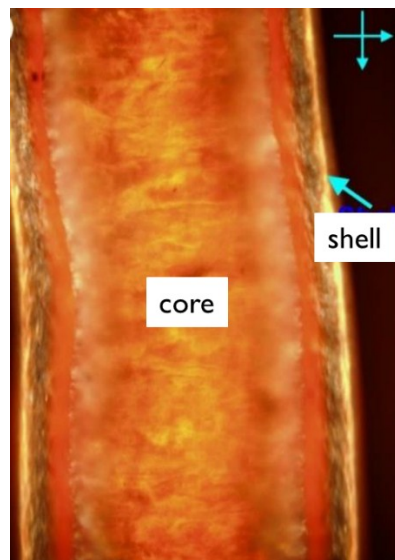


**Figure S4.** Polarized optical microscopy of an as-extruded GO fiber taken at 90°, showing that the coagulation happened at the surface of graphene oxide fibers at the very beginning, resulting in a fiber consisting of a “soft” core and a “hard” shell due to the concentration difference of GO.

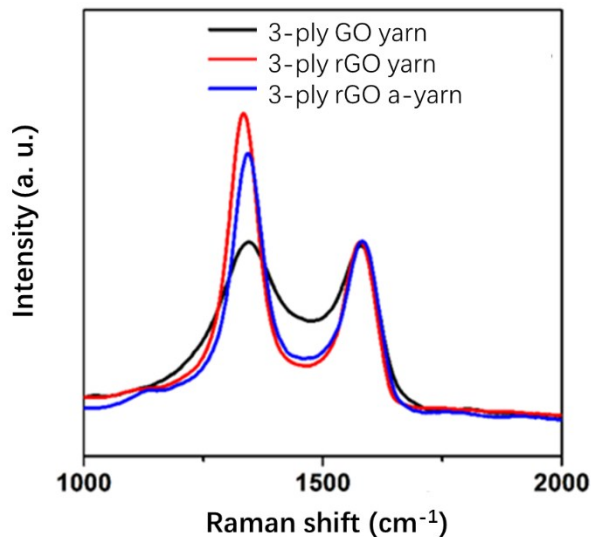


**Figure S5.** Raman spectra showing that rGO yarns prepared by chemical reduction of GO yarns in an aqueous solution of hydroiodic acid before and after yarn drying have quite similar intensity ratio of G/D. The decrease of G/D intensity ratio after reduction could be attributed to the increase of the number of polyaromatic domains with smaller overall size in the r-GO or highly defected carbon lattice after the reduction.<sup>s1</sup>

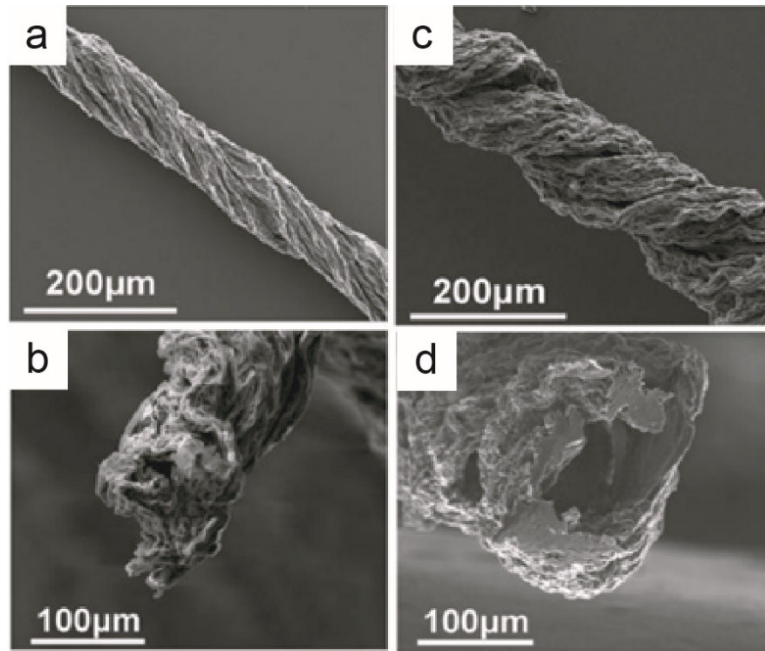


**Figure S6.** Morphological comparison of rGO yarns obtained by chemical reduction of (a,b) air-dried GO yarns and (c,d) as-prepared wet GO yarns.

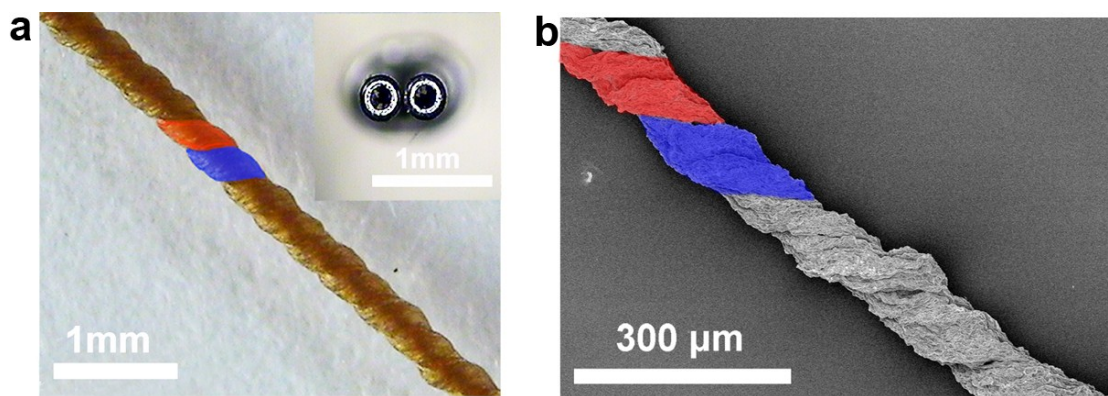


**Figure S7.** (a) Photograph of a double-plied twisted GO yarn. Parts of the individual fibers in yarns were colored for better illustration. (b) SEM image of a double-plied rGO yarn chemically reduced from the GO yarn before air drying, showing that individual fibers were clearly seen and arranged along the yarn axis with a bias angle.

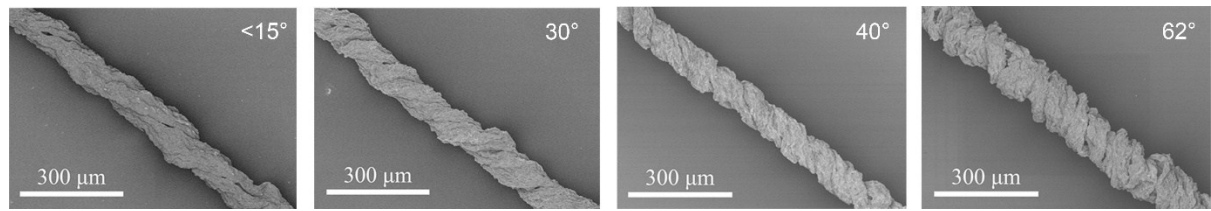


**Figure S8.** SEM images showing double-plied rGO yarns with different bias angles from  $<15^\circ$  to  $62^\circ$ , which was enabled by adjusting the twisting speed of the multi-orifice spinneret and the extruding speed.

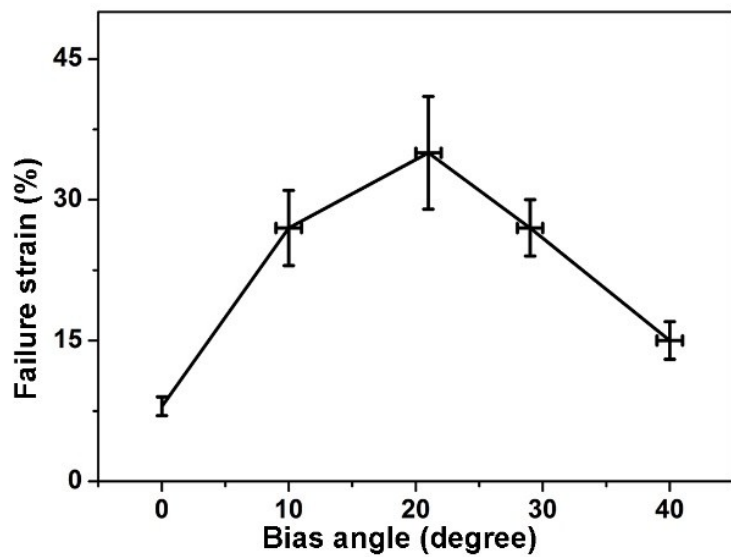


**Figure S9.** Failure strains of a double-plied rGO yarn as a function of bias angles.

#### Reference:

s1. J. I. Paredes, R. S. Villar, F. P. Solis, A. A. Martinez and J. Tascon, *Langmuir*, **2009**, *25*, 5957